

## Original Research Article

# Diffusion Weighted Magnetic Resonance Imaging in Evaluation of Gynecological Masses

### Abstract

**Background:** Diffusion-weighted MRI has potential for tissue differentiation, including cancer. It can also determine cancer histologic type. The ADC value reflects tumor cellular density, allowing tumor grading evaluation. This study aims to assess the role of DW-MRI in gynecological masses.

**Methods:** This prospective cross-sectional research was conducted on 30 female patients between the ages of 20 and 75 who were sent from the gynaecological department to the Radio diagnostic and Medical Imaging department at Tanta University hospitals. All patients gave their informed permission in writing. We included patients with clinically or sonographically suspected uterine and cervical lesions. Patients having indeterminate ultrasonography criteria for adnexal lesions.

**Results:** Resistance index (RI) showed significant predictive value of the malignant masses ( $p=0.13$ ), with an area under curve (AUC) of 0.84. An RI cutoff value of  $\geq 0.365$  could predict malignant masses with a sensitivity of 81.8% and specificity of 87.5%. T ROC curve analysis to assess the validity of ADC to discriminate malignant masses is illustrated. ADC values showed significant predictive value of the malignant masses ( $p<0.001^*$ ), with an area under curve (AUC) of 0.89. An ADC cutoff value of  $\leq 1$  could predict malignant masses with a sensitivity of 85.7% and specificity of 89.5%.

**Conclusions:** Combined ultrasound and MRI examination produced radiologic findings with 98 percent sensitivity, 92.9 percent specificity, 95 percent positive predictive value, and 97 percent negative predictive value when compared to the final pathologic diagnosis. The

research indicated that DWI and ADC mapping are excellent imaging methods for discriminating benign from malignant tumours with a high degree of sensitivity and specificity. However, their effectiveness and benefits depend on a precise diagnosis of the lesions' essential features, such as their origin, size, and composition, as assessed by ultrasound and standard MRI tests.

**Keywords:** Diffusion Weighted Magnetic Resonance Imaging, Gynecological, Masses

## **Introduction:**

Resonance Magnetic Gynaecological lesions are diagnosed by imaging. It facilitates in the identification of ovarian, uterine, and tubal lesions<sup>[1]</sup>. However, traditional Magnetic Resonance Imaging has limitations when it comes to lesion identification and characterization<sup>[2]</sup>. The need to improve tumour and lymph node staging, peritoneal carcinomatosis assessment, tumour response prediction, and post-treatment improvements against disease recurrence has existed for quite some time. New functional imaging sequences, such as diffusion-weighted imaging, have resolved many of these issues and enhanced the diagnostic capabilities of magnetic resonance imaging<sup>[3,4]</sup>.

DWI distinguishes malignant tissue from normal tissue and identifies its histologic type. The Apparent Diffusion Coefficient (ADC) measures tumour cellular density, giving a new pathologic grading technique. Most endometrial lesions share imaging features with normal menstrual phases and endometrial diseases include hyperplasia, polyps, sub mucous fibroid, and carcinoma.<sup>[5,6]</sup>

Vaginal tract neoplasms are the second most prevalent malignancy in women, after breast cancer.<sup>[7]</sup> Endometrial carcinoma, the most common female genital malignancy, is the fourth most common female cancer after ovarian cancer, which is frequently diagnosed late

with extensive peritoneal and lymph node metastases. Cervix cancer is the third most frequent cancer after endometrial and ovarian..<sup>[8]</sup>.

Large screening studies reveal that the majority of adnexal tumours are benign, despite the fact that ovarian cancer is fatal. Benign masses include physiologic cysts, paraovarian masses, and benign ovarian lesions. To avoid unnecessary intervention, gynaecologists and radiologists must comprehend magnetic resonance imaging lesions.<sup>[9]</sup>.

In order to increase lesion characterization and disease mapping, diffusion weighted imaging has been introduced to pelvic magnetic resonance imaging techniques<sup>[10]</sup>. Proton mobility and diffusion-weighted imaging (DWI) are affected by pathological alterations in tissue cellularity, membrane integrity, extracellular space perfusion, and fluid viscosity. Diffusion Weighted is used to detect and characterise cancer lesions, as well as evaluate therapy efficacy. DWI is ideal for individuals with renal failure because to its low cost, short duration, noninvasive nature, absence of ionising radiation, and absence of contrast material injection.<sup>[11]</sup>.

DWI tissue contrast is enhanced by molecular diffusion. Quantitative ADC measurement may also be used to distinguish between malignant and benign tumours..<sup>[12]</sup>.

Before and after the 180° refocusing pulse, T2-weighted DWI employs two equal and opposing gradients for motion detection. The water molecules get phase shift information from the initial gradient pulse and the second gradient, but they are not exposed to the same gradient since they are in motion. Thus, no signal is created at acquisition (free diffusion), but static water molecules (diffusion-restricted) regain signal because the second gradient has not caused a large phase shift and the signal loss from the first gradient is recovered by the second opposing gradient (restricted diffusion).<sup>[13, 14]</sup>.

DWI sequences offer several complications. Unlike normal tissue, tumours with a high cellularity limit diffusion. Blood, fat, necrosis, and pus are all impediments to diffusion. DWI

characteristics of benign and malignant tumours might overlap. Avoid misunderstanding by correlating DWI and ADC data with morphological features.<sup>[12, 15]</sup>

DWI is based on T2W imaging, which allows tissues with a long T2 relaxation period, such as simple cysts, to exhibit a high signal intensity; this phenomenon is known as the T2-shine-through effect. However, an ovarian tumour with a very strong signal on DWI, the ADC map, and T2W pictures — the T2-blackout effect — is probably benign, making DWI the perfect method for ruling out malignancy.<sup>[16]</sup>

This research aims to analyse the effect of Diffusion Weighted Magnetic Resonance Imaging in gynaecological masses of various types.

### **Patients and Methods:**

This prospective cross-sectional research was conducted on 30 female patients between the ages of 20 and 75 who were sent from the gynaecological department to the Radio diagnostic and Medical Imaging department at Tanta University hospitals. All patients gave their informed permission in writing. The research was conducted over the course of one year, from November 2021 to November 2022.

Patients with clinically or ultrasonographically suspected uterine and cervical lesions were included. Patients having ultrasound-detected adnexal lesions that do not meet diagnostic criteria.

We eliminated individuals with general Magnetic Resonance Imaging contraindications (the presence of metallic foreign bodies, pacemakers, aneurysm clips, etc.), those who refused to participate in the study, and those with claustrophobia.

All patients were given a thorough medical history, which included their name, age, smoking status, past medical or surgical history, and menstruation history, including the number of days and quantity of bloodshed. Clinical investigation (vital signs as blood pressure, pulse

rate and complete gynaecological examination). When necessary, laboratory investigation is conducted based on the case.

**Radiological assessment in the form of:**

**1-Pelvi-abdominal and transvaginal ultrasound assessment of the uterus and adnexae was performed.**

**Patient Preparation: An adequate explanation of the procedure to the patient was done.**

The patient's dignity was protected at all times by covering her properly. For the TVS procedure, the pelvis was elevated so that the probe could be angled downwards during the sonographic examination. The patient lay supine with bent knees and flat feet positioned shoulder-width apart on the table.

**Probe Preparation:** A disposable cover, often a latex condom, was put over the probe and attached with rubber bands or other acceptable techniques to avoid cross contamination between patients. The probe was bathed in disinfectant between usage.

After disinfecting and wiping the probe, a tiny quantity of coupling gel should be inserted into the tip of the condom, and the condom should be pushed over the shaft of the probe. Finally, a lubricant was applied to the probe's covered tip to aid entry.

**Scan Technique:** After preparing the probe and the patient, the transducer was inserted gradually while watching the ultrasound picture. The usual consistency of the urine bladder's location in the pelvis compared to the considerably more variable position of the uterus and ovaries makes it a useful marker for early transducer orientation evaluation.

**Three basic scanning manoeuvres of the probe were useful to scan the pelvic organs comprehensively:**

- Sagittal imaging with side-to-side motions
- 90° rotation to get semi-coronal images with probe angulation in vertical plane

- Variation in probe insertion depth to bring various sections inside the field of view/focal zone.

Without aliasing, a Color Doppler investigation was conducted with high sensitivity settings and the lowest feasible pulse repetition frequency. Spectral Doppler imaging was used to analyse the blood arteries identified by colour Doppler tests. Internal vessels were assessed before peripheral vessels where present. The lowest values of pulsatility index (PI) and resistance index (RI) were measured when a repeatable sequence of waveforms was produced..

## **2- MR Imaging for all cases (conventional MRI and DWI):**

Magnetic Resonance and Diffusion-Weighted Imaging for all patients employing Magnetic Resonance Imaging equipment (GE 1.5 tesla) with varied pulse sequences at our Radiodiagnosis department.

### **Patients' preparation**

Patients fasted about 5 hours. 10 mg buscopan (butylscopolamine bromide) was administrated in IV line directly before MRI to decrease bowel peristalsis.

### **MR imaging protocol**

A single shot echo-planar imaging sequence was used to acquire DW Images in axial planes. Lesions were evaluated at various b values: 0, 500, and 1000 sec/mm<sup>2</sup>. Due to the substantial T2 shine-through phenomenon, DWI with b-values of 0 and 500 sec/mm<sup>2</sup> were omitted. ADC values were measured three times in succession. Calculating the average value yields the mean ADC value.

### **Analysis of DWI:**

### **Qualitative analysis:**

The DWI was carried out in the axial oblique plane. We searched for restricted diffusion as evidenced by the presence of persistently high signal intensity at DW images with b value (1000 sec/mm<sup>2</sup>) comparable to signal of normal tissue around, urine or cerebrospinal fluid in adjacent vertebrae and hypointense signal in equivalent ADC map (restricted diffusion) in the solid portion of the involved lesions and signal intensity of the cystic portion of included ovarian lesions.

### **Statistical analysis**

SPSS v27 (IBM, Armonk, NY, USA) was used for statistical analysis. Using the Shapiro-Wilks test and histograms, the normality of the data distribution was determined. Parametric quantitative data were given as mean and standard deviation (SD) and examined using an unpaired student t-test. Non-parametric quantitative data were provided as the median and interquartile range (IQR) and examined using the Mann-Whitney test. When applicable, qualitative variables were given as frequency and percentage (percent) and examined using the Chi-square test or Fisher's exact test. A two-tailed P value of less than or equal to 0.05 was deemed statistically significant. To examine the concordance between the radiological and pathological diagnoses using Kappa agreement.

**6 - Receiver operating characteristic curve (ROC):** It is produced by graphing sensitivity (TP) against 1-specificity (FP) at various cut off levels. The diagnostic performance of a test is represented by the area under the ROC curve. Greater than fifty percent is an acceptable performance on the exam, while about one hundred percent is the greatest possible score. The ROC curve also permits the comparison of the performance of two tests.

### **Results:**

Table 1 showed Socio-demographic and clinical data of the studied patients

**Table 1: Socio-demographic data and menstrual history of the studied patients**

Demographic data (N = 30)		NO.	%
Age (years)			
Min. – Max.		24 – 70	
Mean ± SD.		43.37 ± 12.7	
Median (IQR)		40 (35 – 54)	
Marital status			
Married		25	83.3
Single		5	16.6
Comorbidities			
Hypertension		12	40
Diabetes mellitus		5	16.6
Dyslipidemia		14	46.7
Age of menarche (years)			
Min. – Max.		10 – 16	
Mean ± SD.		12.4 ± 1.4	
Median (IQR)		12 (12 – 13)	
Menopause			
Yes		9	30
No		21	70

**Table 2: Clinical data of the study patients**

Clinical data (N = 30)		NO.	%
Site of the lesion			
Uterine		11	36.7
Location	<b>Endometrial</b>	7	23.3
	<b>Myometrial</b>	4	13.3
Ovarian		19	63.3
Laterality	<b>Right</b>	10	33.3
	<b>Left</b>	6	20
	<b>Bilateral</b>	3	10
Complaint			
Asymptomatic		2	6.7
Vaginal bleeding		23	76.7
Pelvic pain		27	90
Pelvic mass		4	13.3

**Table 3: Ultrasound characteristics of the studied masses (n = 33)**

Ultrasound data	NO.	%
<b>Maximum dimension (cm)</b>		
Min. – Max.	1 – 14	
Mean ± SD.	7.42 ± 4.07	
Median (IQR)	7 (4.2 – 11)	
<b>Echogenicity</b>		
Hyperechoic	2	6.1
Isoechoic	7	21.2
Mixed echogenicity	24	72.7
<b>Doppler vascularity</b>		
Central /nodule/septal vascularity	13	39.4
Peripheral or absent	20	60.6
<b>Resistive index (RI) (n=19)</b>		
< 0.4	12	63
≥ 0.4	7	21.1

**Table 4: MRI characteristics and the final pathological diagnosis of the studied masses (n = 33)**

Ultrasound data	NO.	%
<b>Maximum dimension (cm)</b>		
Min. – Max.	1 – 13	
Mean ± SD.	7.3 ± 3.9	
Median (IQR)	6.2 (4 – 11)	
<b>T1Wi signal</b>		
Low	22	66.7
High	6	18.2
Mixed	5	15.2
<b>T2Wi signal</b>		
Low	7	21.2
High	9	27.3
Mixed	17	51.5
<b>Contrast enhanced MRI</b>		
No enhancement	24	72.7
Mild enhancement	6	18.2
Moderate enhancement	3	9.1
<b>DW-MRI</b>		
Restricted	11	33.3
Free diffusion	18	54.7
T2 shine through	4	12
<b>ADC map</b>		

Low signal	11	33.3
High signal	22	66.7
<b>ADC (<math>\times 10^{-3}</math> mm<sup>2</sup>/sec)</b>		
Min. – Max.	0.13 – 2.9	
Mean $\pm$ SD.	1.27 $\pm$ 0.71	
Median (IQR)	1.25 (0.74 – 1.5)	

Table 4 showed The MRI scan revealed that the masses' maximal dimensions varied from 1 to 13 cm, with a mean of 7.3 3.9 cm. T1wi scans revealed that 22 masses (66.7%) were hypointense, 6 masses (18.2%) were hyperintense, and 5 masses (15.3%) had a mixed signal. 7 masses (21.2 percent) on T2WI images were hypointense, 9 masses (27.3 percent) were hyperintense, and 17 masses (51.5 percent) had a mixed signal. At CE-MRI, the majority of masses were non-enhanced (24 masses; 72.7 percent), followed by 6 masses with mild enhancement (18.2 percent) and 3 masses with moderate enhancement (3.1 percent) (9i.1 percent ). 11 masses (33.3% of the total) exhibited diffusion limitation on DW-MRI, whereas 18 masses (54.7% of the total) exhibited free diffusion and 4 masses (12%) exhibited T2 shine through phenomena. ADC mapping indicated that 11 masses (33.3%) had a low signal level, whereas 22 masses (66.7%) had a high signal level. The masses ADC varied from 0.13 to 2.9 (10<sup>-3</sup> mm<sup>2</sup>/sec), with a mean value of 1.27 0.71 (10<sup>-3</sup> mm<sup>2</sup>/sec) based on the radiological diagnostic of the masses.

**Table 5: Radiological and Pathological diagnosis of the studied pelvic masses (n = 33)**

	<b>Radiologic diagnosis</b>		<b>Pathological diagnosis</b>	
	No.	%	No.	%
<b>Type of the mass (n = 33)</b>				
Benign	20	60.6	19	57.6
Malignant	13	29.4	14	42.4
<b>Ovarian masses</b>				
Serous cystadeocarcinoma	6	18.2	5	15.2
Mucinous cystadenoma	5	15.2	1	3
Mucinous cystadenocarcinoma	4	12.2	5	15.2

Serous cystadenoma	2	6.1	4	12.2
Dermoid cyst	2	6.1	1	3
Tubo-ovarian abscess	1	3	2	6.1
Endometrioma	1	3	2	6.1
Fibroma	1	3	1	3
Clear cell carcinoma	-	-	1	3
<b>Uterine masses</b>				
Leiomyoma	4	12.2	4	12.2
Endometrial carcinoma	3	9.1	4	12.2
Endometrial polyp	2	6.1	1	3
Endometrial hyperplasia	1	3	1	3
Adenomyosis	1	3	1	3

Twenty masses seemed to be benign (60.6%), whereas thirteen appeared to be malignant. 22 masses were of ovarian origin (66.7%), whereas 11 were uterine (11.3%). (33.3 percent ). Concerning radiologic diagnosis, the ovarian masses were serous cystadenocarcinoma (6 masses; 18.2 percent), mucinous cystadenoma (5 masses; 15.2 percent), mucinous cystadenocarcinoma (4 masses; 12.2 percent), serous cystadenoma and dermoid cyst (2 masses each; 6.1 percent), tubo-ovarian abscess, endometrioma, and fibroma (one lesion each; 3 percent ). As for uterine masses, four were leiomyomas (12.2%), three were endometrial cancer (9.1%), two were endometrial polyps (6.1%), one was endometrial hyperplasia (3%) and another was adenomyosis (3%). (3 percent ). Table 5 details the conclusive pathology diagnosis. 19 masses (56.6 percent) were of benign type, whereas 14 masses were of malignant nature (42.4 percent ). 22 masses were of ovarian origin (66.7%), whereas 11 were uterine (11.3%). (33.3 percent ). Concerning tissue types, this was comparable to the radiological diagnosis with the exception of two cases in which the radiological diagnostic of serous cystadenocarcinoma was replaced by clear cell carcinoma and endometrial polyp was replaced by endometrial carcinoma.

**Table 6: Comparison between patients with benign and malignant masses according to sociodemographic and clinical data**

	PATIENTS WITH		TEST OF SIG.	P
	Benign mass (n = 18)	Malignant mass (n = 12)		
Age (years)				
Mean ± SD.	38.1 ± 7.03	47.25 ± 17.15	t = 2.1	0.05*
Marital status: n (%)				
Married	17 (94.4)	7 (58.3)	$\chi^2=5.9$	0.015*
Single	1 (5.6)	5 (41.7)		
Site: n (%)				
Uterine	7 (38.9)	4 (33.3)	$\chi^2=0.76$	0.096
Ovarian	11 (61.1)	8 (66.7)		
Complaint: n (%)				
Vaginal bleeding	16 (88.9)	7 (58.3)	Z=1.9	0.052
Pelvic pain	17 (94.4)	10 (83.3)	Z=-0.99	0.32
Pelvic mass	3 (16.7)	0 (0)	Z=1.5	0.14
Menopause: n (%)				
Premenopausal	16 (88.9)	6 (50)	$\chi^2=5.6$	0.018*
Postmenopausal	2 (11.1)	6 (50)		
Mass laterality: n (%)				
Bilateral	1 (5.6)	2 (16.7)	$\chi^2=0.32$	0.99
Unilateral	17 (94.4)	10 (83.3)		

t: Student t-test,  $\chi^2$ : Chi-square test, Z: Z test for proportion, SD: Standard deviation, \*: Statistically significant at  $p \leq 0.05$

Table 6 showed that it was found that patients with malignant masses had significantly higher age ( $47.25 \pm 17.15$  compared to  $38.1 \pm 7.03$ ), with a p value of 0.05\*. Significantly higher percentage of single women (41.7% compared to 5.6%), with a p value of 0.015, and significantly higher percentage of postmenopausal women (50% compared to 11.1%), with a p value of 0.018\*

**Table 7: Comparison between ultrasound & Doppler findings in benign and malignant masses**

	MASS		TEST OF SIG.	P
	Benign (n = 20)	Malignant (n = 13)		
Largest diameter (cm)				
Mean ± SD.	6.5 ± 3.8	8.7 ± 4.03	t = 1.3	0.2
Site: n (%)				
Uterine	8 (40)	3 (23.1)	$\chi^2=1.06$	0.31

Ovarian	12 (60)	10 (76.9)		
Echogenicity: n (%)				
Mixed	14 (70)	10 (76.9)		0.02* <sup>F</sup>
Hyperechoic	0 (0)	2 (15.4)		
Isoechoic	6 (30)	1 (7.8)		
Vascularity: n (%)				
Central /nodule/septal vascularity	3 (15)	10 (76.9)	$\chi^2=12.7$	<0.001*
Peripheral or absent	17 (85)	3 (23.1)		
Mass laterality: n (%)				
Bilateral	2 (10)	4 (30.8)	$\chi^2=2.3$	0.13
Unilateral	18 (90)	9 (69.2)		
Resistive index (n=19)				
>0.4	1 (5)	6 (46.2)	$\chi^2=4.87$	0.027*
<0.4	8 (40)	4 (30.8)		

t: Student t-test,  $\chi^2$ : Chi-square test, F: Fisher exact test, SD: Standard deviation, \*: Statistically significant at  $p \leq 0.05$

Table 7 Comparison between ultrasound data of benign and malignant masses showed that there was statistically significant differences between benign and malignant masses in the distribution of ultrasound echogenicity, with higher frequency of mixed appearance of malignant lesions ( $p=0.02^*$ ), in the Doppler vascularity distribution, with higher frequency of central/nodule/septal vascularity in malignant masses ( $p<0.001^*$ ), and in the distribution of RI categories, with higher percentage of malignant masses showing  $RI > 0.04$  ( $p=0.027^*$ )

**Table 8: Validity of RI and ADC to discriminate malignant masses**

	AUC	P	95% C.I	CUTOFF	SENSITIVITY	SPECIFICITY
RI	0.84	0.013*	0.66 – 1	$0.365 \leq$	81.8%	%87.5
ADC	0.89	>0.001*	0.77– 1	$\leq 1$	85.7%	%89.5

AUC: Area Under a Curve, CI: Confidence Intervals, \*: Statistically significant at  $p \leq 0.05$ .

Table 8 showed ROC curve analysis to assess the validity of RI to discriminate malignant masses is illustrated. RI showed significant predictive value of the malignant masses ( $p=0.13$ ), with an area under curve (AUC) of 0.84. An RI cutoff value of  $\geq 0.365$  could predict malignant masses with a sensitivity of 81.8% and specificity of 87.5%. T ROC curve analysis to assess the validity of ADC to discriminate malignant masses is illustrated. ADC values showed significant predictive value of the malignant masses ( $p<0.001^*$ ), with an area under curve (AUC) of 0.89. An ADC cutoff value of  $\leq 1$  could predict malignant masses with a sensitivity of 85.7% and specificity of 89.5%.

**Table 9: Comparison between MRI data of benign and malignant masses**

	MASS		TEST OF SIG.	P
	Benign (n = 20)	Malignant (n = 13)		
<b>T1WI signal: n (%)</b>				
High	4 (20)	2 (15.4)	$\chi^2=4.2$	0.24
Intermediate	1 (5)	3 (23.1)		
Low	15 (75)	7 (53.8)		
<b>T2WI signal: n (%)</b>				
Heterogenous	9 (45)	8 (61.5)	$\chi^2=1.7$	0.4
High	9 (45)	3 (23.1)		
Low	2 (10)	2 (15.4)		
<b>CE-MRI: n (%)</b>				
Mild enhancement mass	3 (15)	0 (0)	$\chi^2=6.6$	0.038*
Moderate enhancement (nodule/stations)	0 (0)	9 (69.2)		
No enhancement	17 (85)	4 (30.8)		
<b>DW-MRI: n(%)</b>				
Free diffusion	15 (75)	3 (23.1)	$\chi^2=12.5$	0.002*
Restricted	2 (10)	9 (69.2)		
T2 shine through	3 (15)	1 (7.7)		
<b>ADC map: n(%)</b>				
Low signal	2 (10)	9 (69.2)	$\chi^2=12.44$	<0.001*
High signal	18 (90)	4 (30.8)		
<b>ADC (<math>\times 10^{-3}</math> mm<sup>2</sup>/sec)</b>				
Mean $\pm$ SD.	1.6 $\pm$ 0.67	0.76 $\pm$ 0.43	t = 4	<0.001*

t: Student t-test,  $\chi^2$ : Chi-square test, F: Fisher exact test, SD: Standard deviation, \*: Statistically significant at  $p \leq 0.05$

Table 9 demonstrate that malignant masses had significantly lower mean ADC values (0.76  $\pm$  0.43 vs. 1.6  $\pm$  0.67), with a p value of <0.001\*. Also, malignant masses differed significantly in the pattern of enhancement, DW, and ADC map signal, with higher percentage of enhancement (p=0.038\*), diffusion restriction in DWI (p=0.002\*) and ADC map (p<0.001).

**Table 10: Specificity, sensitivity, positive predictive value, negative predictive value, and Kappa agreement of the radiological diagnosis compared to the pathological diagnosis**

		PATHOLOGICAL DIAGNOSIS	
		Benign	Malignant
Radiological diagnosis	Benign	19	1
	Malignant	0	13
Sensitivity		98%	
Specificity		92.9%	
Positive predictive value		95%	
Negative predictive value		97%	
Kappa agreement		0.93 (Substantial agreement)	
P		<0.001	

Table 10 Comparison between the radiologic diagnosis and the final pathologic diagnosis. The radiologic diagnosis showed 98% sensitivity, 92.9% specificity, 95% positive predictive value, and 97% negative predictive value compared to the final pathologic diagnosis. There was substantial agreement between both, with kappa value of 0.93 and  $p < 0.001$ .

## Discussion

On each side of the  $180^\circ$  refocusing pulse, diffusion sensitization gradients are given to the DWI sequence. The parameter "b value," which is stated in  $\text{mm}^2/\text{sec}$ , determines the diffusion weighting. It is proportional to the square of the amplitude and duration of the gradient applied. Diffusion is measured intuitively using trace pictures and quantitatively using the apparent diffusion coefficient parameter (ADC). Tissues with restricted diffusion are bright on the trace image and hypointense on the ADC map<sup>[17]</sup>.

Both gradients should cancel each other, and the tissue with restricted diffusion will be fully rephased, preserving its T2 signal intensity, whereas in the tissue with free diffusion, the water molecules would move significantly between the two gradients and not be fully rephased, resulting in a decrease in T2 signal intensity.<sup>[18]</sup>

DW-MRI can describe tissues in terms of cell organisation and density, microstructure, and microcirculation based on the water diffusion parameters associated with each of these characteristics<sup>[19]</sup>.

Other individuals for whom gadolinium is contraindicated, such as those with renal disease, may benefit from DWI. DWI not only improves the identification and perhaps the characterisation of tiny uterine tumours and complicated ovarian cancer, but also the visibility of small implants of peritoneal carcinomatosis, which might have a substantial influence on patient care<sup>[20]</sup>.

The topic of oncoimaging offers enormous promise for diffusion-weighted imaging. It is straightforward to install and adds little time to a normal MR test. In cancers of the brain, head and neck, prostate, and liver, malignant lesions have lower ADC values than surrounding normal tissue, edoema, or benign tumours. The cellularity and biological aggressiveness of malignant tumours may be evaluated by their ADC values<sup>[17]</sup>. DWI of the whole body, i.e. diffusion-weighted imaging of the entire body with background suppression (DWIBS), is achieved utilising a STIR EPI sequence with a high b value for background suppression. Multiple stations produce imaging, which is subsequently post-processed to create a composite picture of the whole body. The images are shown as maximum intensity projections with the grayscale inverted. Except for the prostate, spleen, ovaries, testes, spinal cord, and endometrium, signals from the bulk of normal tissues are silenced. Areas exhibiting limited diffusion, such as highly cellular lymph nodes, are emphasised in a dramatic manner. Using this method, small tumour foci in the abdomen or peritoneum may also be emphasised. Recent uses of DWI in cancer include chemoradiotherapy response assessment. An increase in ADC value may be seen before the tumour diminishes in size.<sup>[21]</sup>

Majority of gynecological masses in the current study were ovarian (66.7%), while uterine masses were 33.3% of cases that is consistent with **Sharma et al. (2019)**<sup>[19]</sup> who reported that

ovarian masses represented 66% of the diagnosed gynecological masses. **Cass and Newton (2020)**<sup>[22]</sup> also This is probable because the majority of uterine lumps are leiomyomas, which are asymptomatic and do not prompt patients to seek medical attention.

In the current study, 19 masses were of benign nature (57.6%), while 14 masses were of malignant nature (42.4%). This is in line with the study of **Abd-Elmageed et al. (2021)**<sup>[20]</sup> and **El-Sayed et al. (2019)**<sup>[18]</sup> who showed that benign masses were more prevalent than malignant masses. This was also confirmed in the meta-analysis conducted by **Guo et al. (2021)**<sup>[23]</sup> on 2474 patients and reported higher prevalence of benign masses.

The present investigation revealed that patients with malignant tumours were substantially older and had a greater proportion of postmenopausal women. Likewise, **Rai et al. (2019)**<sup>[21]</sup> found that women above 50 years were shown to have significantly increased risk of ovarian malignancy, and also reported significant association among women of menopausal group and malignancy. Similar findings were reported by **Rai et al. (2016)**<sup>[24]</sup>, **Karimi-Zarchi et al. (2015)**<sup>[25]</sup> and **Terzic et al. (2013)**<sup>[26]</sup>.

The present study showed that patients with malignant masses were more prevalently single women. This may be attributed to issue of hormonal changes, or psychological stress. In agreement with this findings, the recent study of **Alamri et al. (2021)**<sup>[27]</sup> reported that a single marital status was a significant predictor of lesion malignancy.

There were statistically significant differences between benign and malignant masses in the distribution of ultrasound echogenicity, with a higher frequency of mixed appearance in malignant lesions, and in the distribution of Doppler vascularity, with a higher frequency of central/nodule/septal vascularity in malignant masses (13 cases, 39.4 percent ). These data illustrate the behaviour of malignant tissue proliferation, which is marked by chaotic development, papillary projections, and aberrant angiogenesis. These findings were in harmony with findings of **Rauh-Hain et al. (2015)**<sup>[28]</sup> who noticed that complex

multiloculated cysts and partially solid cysts were associated with high risk of malignancy. In addition, **Lovely and Rajesh (2013)**<sup>[29]</sup> reported that all malignant ovarian tumors were showing cystic mass with ill-defined walls and solid component.

Doppler evaluation of resistance index (RI) in this research revealed a considerably greater proportion of malignant tumours with  $RI > 0.40$ . In addition, a RI cutoff value of 0.365 demonstrated considerable predictive value for malignant masses with an area under the curve (AUC) of 0.84, a sensitivity of 81.8% and a specificity of 87.5%. The predictive power of RI in discrimination of malignant lesions was comparable to findings of **Neeyalavira et al. (2008)**<sup>[30]</sup> where mean RI in the benign and malignant group was significantly different, and the mean RI of malignant lesions was 0.44. **Majeed et al. (2011)**<sup>[31]</sup> confirmed the validity of RI to diagnose malignant lesions, with most of the malignant masses' RI was above 0.4. recently, The study by **Abbas et al. (2014)**<sup>[32]</sup> also revealed that using 0.42 for RI as a cutoff value for prediction of malignancy.

In this study, the differences between benign and malignant masses on conventional MRI images (T1WI and T2WI sequences) were not statistically significant; however, there were statistically significant differences in contrast enhancement, signal intensity in DWI (at 1000 mm<sup>2</sup>/sec), and ADC images, ADC values. In addition, malignant masses had considerably lower mean ADC values, with an ADC cut-off value of 1 demonstrating strong predictive value with an AUC of 0.89, sensitivity of 85.7 percent, and specificity of 89.5 percent. In the current investigation, the majority of malignant lesions (69.2 percent) exhibited moderate enhancement as nodular and septation enhancement. In consistency with this study findings, the recent Egyptian studies of **El-Sayed et al. (2019)**<sup>[18]</sup>, **Mansour et al. (2020)**<sup>[33]</sup>, **Hamed et al. (2021)**<sup>[34]</sup> and **Abd-Elmageed et al (2021)**<sup>[20]</sup> reported that the appearance of benign and malignant lesions was rather similar in T1WI and T2WI, but as regarding contrast

enhancement, the gynecological masses showed different pattern of enhancement according being benign or malignant.

In line with the present study, there was an initial experience in 2004, conducted by **Sarty et al.**<sup>[124]</sup> and only 12 cases were examined to assess the viability of ADC measurement for the differential diagnosis of cancer. The conclusion of the research was that ADC measurement, intensity, and texture may identify malignancy in ovarian tumours. In addition, **El-Sayed et al. (2019)**<sup>[181]</sup>, **Mansour et al. (2020)**<sup>[33]</sup>, **Hamed et al. (2021)**<sup>[34]</sup> and **Abd-Elmageed et al (2021)**<sup>[20]</sup> reported that although some overlaps were found in the ADC values of benign and malignant lesions, yet the mean ADC value of malignant masses was significantly lower than that of benign, which is similar to current study. **Thomassin-Naggara et al. (2009)**<sup>[35]</sup> evaluated the contribution of DWI in conjunction with morphological criteria to characterize gynecological masses. In their results, appearance on DWI would help in differentiating benign from malignant lesion. This was also found in the study of **Zhang et al. (2012)**<sup>[36]</sup> who showed that DWI appears to be a useful method for differentiating between benign and malignant tumors. In contrary to this study findings, **Inci et al. (2011)**<sup>[37]</sup> study declared that the ADC values of benign and malignant lesions overlap and DWI cannot be used for discrimination. This discrepancy in findings resulted from that the authors did not consider the DWI pitfalls. In addition, they included large number of benign cystic lesions those are known to cause diffusion restriction and low ADC values, such as endometriomas, hemorrhagic cysts and dermoid cysts.

In variance with this study findings, the recent Egyptian study of **Ali et al. (2020)**<sup>[38]</sup> Combining DWI with standard MRI sequences revealed a poor sensitivity (71,4 percent) for discriminating malignant adnexal masses. The authors explained that this low specificity was due to the presence of eight false-positive cases (eight benign adnexal masses that mimicked malignancy), including necrotizing caseating granuloma, mature cystic

teratomas, infarcted ovary, and cyst-adenofibroma, which were excluded from the current study.

The majority of ovarian masses were benign cysts, according to the final pathology diagnosis (12 masses; 36.5 percent: 5 masses of mucinous cystadenoma, 2 masses of serous cystadenoma, 2 dermoid cysts, 1 tubo-ovarian abscess, and 1 endometrioma). In the meanwhile, the benign ovarian solid lesion was fibroma (in one case only, 3 percent ). Malignant ovarian lesions were predominantly serous cystadenocarcinoma (5 masses; 15.2 percent), mucinous cystadenocarcinoma (4 masses; 12.2 percent), and clear cell carcinoma (1 mass; 3 percent ). In keeping with these results, **Lovely and Rajesh (2013)**<sup>[29]</sup> reported that the most common ovarian masses were benign cystic lesions (43%), and the most common ovarian malignancy was serous cystadenocarcinoma. Also **Rai et al. (2019)**<sup>[21]</sup> demonstrated that the highest percentage of malignant ovarian were epithelial ovarian cancers.

Concerning uterine lesions, the highest percentage were leiomyomas (12.2%), and endometrial carcinoma (9.1%). Other lesions were endometrial polyp (6.1%), endometrial hyperplasia (3%), and adenomyosis (3%). Similarly, **Abd-Elmageed et al (2021)**<sup>[20]</sup> and **Sharma et al. (2019)**<sup>[19]</sup> found that the most prevalent benign tumors were leiomyomas. This is also consistent with the well documented data that uterine leiomyomas are the most prevalent benign pelvic tumor in women.

The current work showed that the radiologic findings obtained from the ultrasound and MRI examinations showed 98% sensitivity, 92.9% specificity, 95% positive predictive value, and 97% negative predictive value compared to the final pathologic diagnosis. There was substantial agreement between both as shown from the kappa value. In congruence with these findings, the study of **Crestani et al. (2020)**<sup>[39]</sup> who assessed the benefits of combining ultrasound and MRI in the evaluation of adnexal masses compared to each modality

individually, and observed that the highest sensitivity and specificity was obtained by their combination.

The findings of this research indicated that DWI and ADC map seems to be an effective strategy for distinguishing benign from malignant ovarian tumours and is linked with a high degree of sensitivity and specificity. However, their usage and advantages are contingent on a correct diagnosis of the fundamental features of the lesions, such as their origin, size, and composition.

**Conclusion:** Combined ultrasound and MRI scans yielded radiological results with 98 percent sensitivity, 92.9 percent specificity, 95 percent positive predictive value, and 97 percent negative predictive value relative to the final pathologic diagnosis. This research revealed that DWI and ADC map seem to be a beneficial imaging modality for distinguishing benign from malignant tumours and are linked with a high degree of sensitivity and specificity. However, their usage and advantages depend on the accurate identification of the fundamental features of the lesions, such as their origin, size, and composition, as determined by ultrasound and standard MRI scan. MRI examinations of patients with gynaecological masses should include a standard sequence of diffusion weight assessment. Additionally, in-depth research with a broader sample of the population should be conducted.

## **References:**

1. Lupean RA, Ștefan PA, Csutak C, Lebovici A, Măluțan AM, Buiga R, et al. Differentiation of Endometriomas from Ovarian Hemorrhagic Cysts at Magnetic Resonance: The Role of Texture Analysis. *Medicina (Kaunas)*. 2020;56:78-92.
2. Nougaret S, Nikolovski I, Paroder V, Vargas HA, Sala E, Carrere S, et al. MRI of Tumors and Tumor Mimics in the Female Pelvis: Anatomic Pelvic Space-based Approach. *Radiographics*. 2019;39:1205-29.

3. Duarte AL, Dias JL, Cunha TM. Pitfalls of diffusion-weighted imaging of the female pelvis. *Radiol Bras.* 2018;51:37-44.
4. Addley H, Moyle P, Freeman S. Diffusion-weighted imaging in gynaecological malignancy. *Clin Radiol.* 2017;72:981-90.
5. Yajima R, Kido A, Kurata Y, Fujimoto K, Nakao KK, Kuwahara R, et al. Diffusion-weighted imaging of uterine adenomyosis: Correlation with clinical backgrounds and comparison with malignant uterine tumors. *J Obstet Gynaecol Res.* 2021;47:949-60.
6. Stolyarova IV, Yakovleva EK, Sharakova VV. [Evaluation of diagnostic effectiveness of the method of diffusion-weighted MR-images in diagnosis of pathology of the uterine body]. *Vopr Onkol.* 2015;61:986-93.
7. Abd El Hafeez MN, Ahmed EA, Mohammad EM, El Sayed HA, Abdel-Tawab M. Role of diffusion-weighted magnetic resonance imaging in the characterization of uterine neoplasms. *Curr Med Res Pract.* 2020;5:33-7.
8. Keriakos NN, Darwish E. Diffusion weighted imaging in suspicious uterine tumors; how efficient is it? *Egypt J Radiol Nucl Med.* 2018;49:838-45.
9. El-Sayed E-SM, Abdullah MS, Ali HG. The role of diffusion-weighted MRI on the differentiation of complex adnexal masses. *Menoufia Medical Journal.* 2019;32:881.
10. Ali RF, Nassef HH, Ibrahim AM, Chalabi NAM, Mohamed AM. The Role of Diffusion Weighted Imaging in suspected cases of ovarian cancer. *Egyptian Journal of Radiology and Nuclear Medicine.* 2020;51:1-11.
11. Türkoğlu S, Kayan M. Differentiation between benign and malignant ovarian masses using multiparametric MRI. *Diagn Interv Imaging.* 2020;101:147-55.
12. Abd Elsamie HA, El-Rasheedy MI, Mohammed MA. Evaluating the role of MRI with diffusion-weighted images in diagnosis of uterine focal lesions. *Al-Azhar Assiut Medical Journal.* 2019;17:103.

13. Osman NM, Mourad MA-f. The value of the added diffusion-weighted images to multiparametric MRI in the early diagnosis of uterine cervix cancers and nodal assessment. *Egypt J Radiol Nucl Med.* 2021;52:1-8.
14. Elsammak A, Shehata S, Abulezz M, Gouhar G. Efficiency of diffusion weighted magnetic resonance in differentiation between benign and malignant endometrial lesions. *Egypt J Radiol Nucl Med.* 2017;48:751-9.
15. Dimova J, Zlatareva D, Bakalova R, Aoki I, Hadjidekov G. Adnexal masses characterized on 3 tesla magnetic resonance imaging - added value of diffusion techniques. *Radiol Oncol.* 2020;54:419-28.
16. Agostinho L, Horta M, Salvador JC, Cunha TM. Benign ovarian lesions with restricted diffusion. *Radiol Bras.* 2019;52:106-11.
17. Dhanda S, Thakur M, Kerkar R, Jagmohan P. Diffusion-weighted imaging of gynecologic tumors: diagnostic pearls and potential pitfalls. *Radiographics.* 2014;34:1393-416.
18. El-Sayed E-SM, Abdullah MS, Ali HG. The role of diffusion-weighted MRI on the differentiation of complex adnexal masses. *Menoufia Med J.* 2019;32:881.
19. Sharma H, Kumar M, Pandey A, Kumar L, Nishi N. Gynaecological Pelvic Masses: A Clinical Challenge – Radiological Evaluation using Ultrasound and CT with Pathological Correlation. *Int J Contemp Med.* 2019;4:148-87.
20. Abd-Elmageed MK, Mohamed RA, Elaziz Maaly MA. Role of MRI Diffusion Weighted Imaging in Evaluation of Gynecological Pelvic Masses. *Egypt J Hosp Med.* 2021;85:3857-64.
21. Rai R, Bhutia PC, Tshomo U. Clinicopathological profile of adnexal masses presenting to a tertiary-care hospital in Bhutan. *South Asian J Cancer.* 2019;8:168-72.
22. Cass GK, Newton C. The pelvic mass: assessment and evaluation. *Obstet Gynaecol Reprod Med.* 2020;30:139-45.

23. Guo W, Zou X, Xu H, Zhang T, Zhao Y, Gao L, et al. The diagnostic performance of the Gynecologic Imaging Reporting and Data System (GI-RADS) in adnexal masses. *Ann Transl Med.* 2021;9:39-58.
24. Rai R, Bhutia PC, Tshomo U. Clinicopathological profile of adnexal masses presenting to a tertiary-care hospital in Bhutan. *South Asian J Cancer.* 2019;8:168-72.
25. Karimi-Zarchi M, Mojaver SP, Rouhi M, Hekmatimoghaddam SH, Moghaddam RN, Yazdian-Anari P, et al. Diagnostic Value of the Risk of Malignancy Index (RMI) for Detection of Pelvic Malignancies Compared with Pathology. *Electron Physician.* 2015;7:1505-10.
26. Terzic MM, Dotlic J, Likic I, Ladjevic N, Brndusic N, Arsenovic N, et al. Current diagnostic approach to patients with adnexal masses: which tools are relevant in routine praxis? *Chin J Cancer Res.* 2013;25:55-62.
27. Alamri F, Abdelfattah EH, Sait K, Anfinan NM, Sait H. Building a Predictive Model for Gynecologic Cancer Using Levels of Data Analytics. *Academic Journal of Applied Mathematical Sciences.* 2021;7:192-7.
28. Rauh-Hain JA, Melamed A, Buskwofie A, Schorge JO. Adnexal mass in the postmenopausal patient. *Clin Obstet Gynecol.* 2015;58:53-65.
29. Lovely K, Rajesh M, Kaushal L. Real Time Ultrasonographic Evaluation of Gynecological Pelvic Masses-a Prospective Study. *J Evol Med Den Sci.* 2013;2:47-83.
30. Neeyalavira V, Tongsong T, Wanapirak C. Doppler indices for prediction of benign and malignant ovarian tumor. *Thai J Obstet Gynaecol.* 2008;84:55-63.
31. Majeed H, Ramzan A, Imran F, Mahfooz ur R. Validity of resistive index for the diagnosis of malignant ovarian masses. *J Pak Med Assoc.* 2011;61:1104-7.

32. Abbas AM, Zahran KM, Nasr A, Kamel HS. A new scoring model for characterization of adnexal masses based on two-dimensional gray-scale and colour Doppler sonographic features. *Facts Views Vis Obgyn.* 2014;6:68-74.
33. Mansour TM, Tawfik MH, El-Barody MM, Sileem SA, Okasha A. Correlation between ultrasound and Magnetic Resonance Imaging in diagnosis of Ovarian Tumors. *Al-Azhar Int Med Jo.* 2020;1:214-23.
34. Hamed MK, Aborashed AA, Ria HFA, Tawfik MH. Ultrasound and diffusion MRI in evaluation of ovarian lesions. *Scientific J Al-Azhar Med Faculty Girls.* 2021;5:90-1.
35. Forstner R, Thomassin-Naggara I, Cunha TM, Kinkel K, Masselli G, Kubik-Huch R, et al. ESUR recommendations for MR imaging of the sonographically indeterminate adnexal mass: an update. *Eur Radiol.* 2017;27:2248-57.
36. Zhang H, Zhang GF, Wang TP, Zhang H. Value of 3.0 T diffusion-weighted imaging in discriminating thecoma and fibrothecoma from other adnexal solid masses. *J Ovarian Res.* 2013;6:58-9.
37. Inci E, Kilickesmez O, Hocaoglu E, Aydin S, Bayramoglu S, Cimilli T. Utility of diffusion-weighted imaging in the diagnosis of acute appendicitis. *European radiology.* 2011;21:768-75.
38. Ali RF, Nassef HH, Ibrahim AM, Chalabi NAM, Mohamed AM. The Role of Diffusion Weighted Imaging in suspected cases of ovarian cancer. *Egypt J Radiol Nucl Med.* 2020;51:1-11.
39. Crestani A, Theodore C, Levailant JM, Thomassin-Naggara I, Skalli D, Miailhe G, et al. Magnetic Resonance and Ultrasound Fusion Imaging to Characterise Ovarian Masses: A Feasibility Study. *Anticancer Res.* 2020;40:4115-21.

**Cases:**

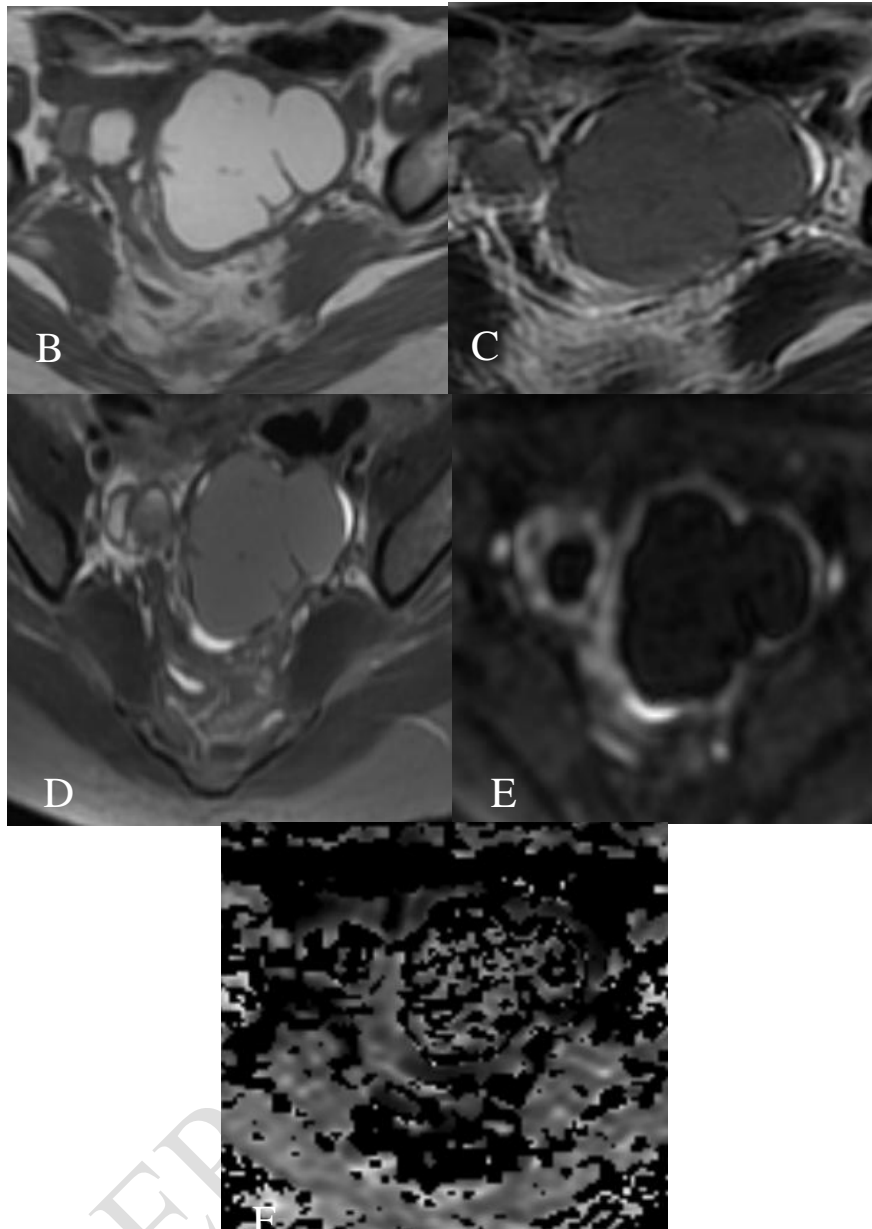
**Case (1)**

(A) thirty-six years old patient complaining of left iliac fossa pain and irregular vaginal bleeding.



**I- Trans-abdominal B-mode ultrasound image shows:**

Left adnexal oblong shaped cystic lesion measures about 6.5x5cm with fine septations and no vascularity on color Doppler study, fine internal echoes seen within it.



**II- MRI shows:**

**(B) Axial T1WI** left adnexal multilocular cystic lesion of high signal intensity.

**(C) Axial T2WI** display low signal intensity.

**(D)STIR** sequence displays low signal (acute to subacute blood signal).

**(E)DW-MRI with  $b= 1000 \text{ sec/ mm}^2$**  shows low signal intensity (free diffusion).

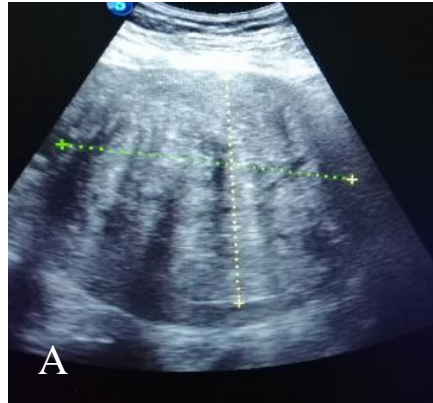
**(F)ADC map image** demonstrates intermediate to low signal intensity on the corresponding ADC map with ADC value ( $1.287 \times 10^{-3} \text{ mm}^2/\text{s}$ ).

**Radiological diagnosis:** Benign looking adnexal lesion likely hemorrhagic cyst.

**Pathological diagnosis:** Left ovarian hemorrhagic cyst confirmed after laparoscopy).

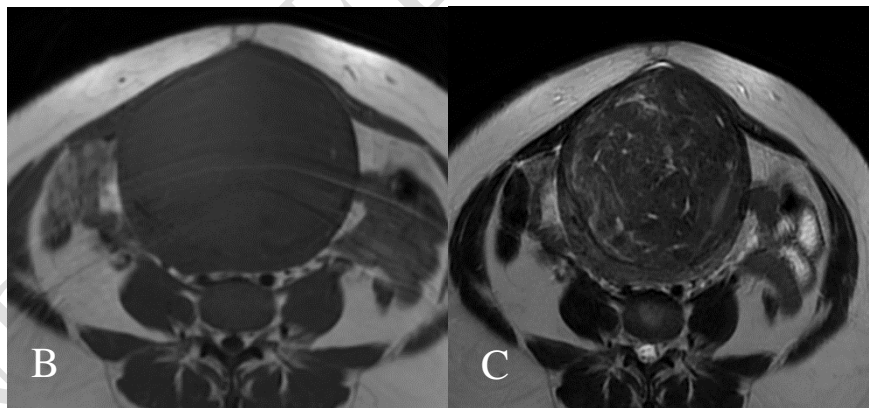
**Case (2)**

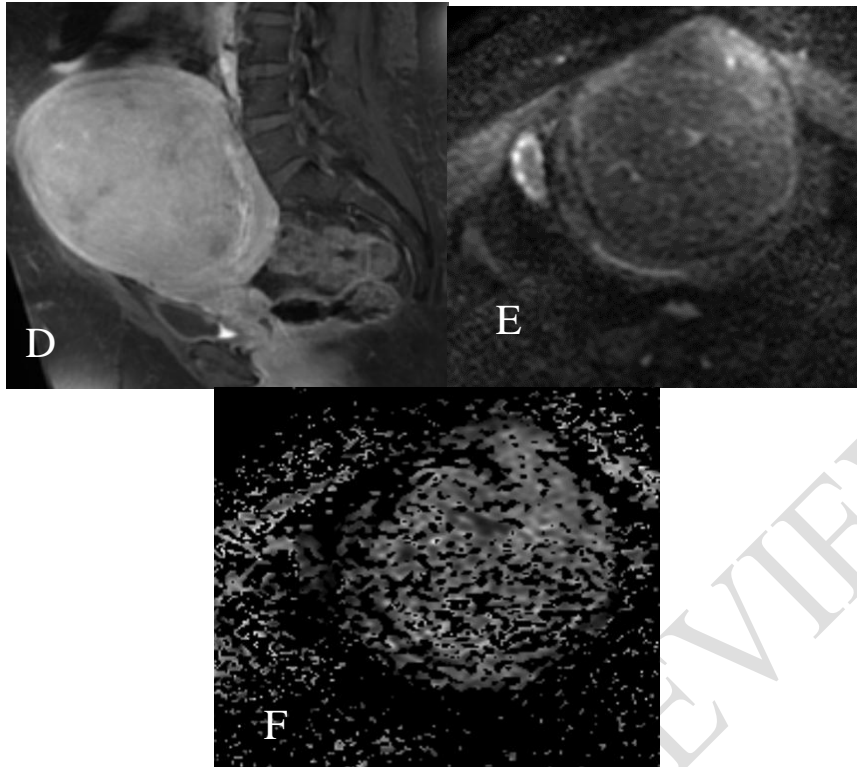
A forty-one years old Female patient presented with chronic pelvic pain, dyspareunia and menorrhagia.



**I-Trans-abdominal B-mode ultrasound image shows:**

(A) well-defined large heterogenous rounded shaped pelvi-abdominal soft tissue mass being inseparable from anterior uterine wall with whorly appearance and internal hypoechoic areas of cystic degenerations, the lesion measures about (11x11cm).





## II- MRI finding:

**(B) Axial T1WI** shows large pelvi-abdominal soft tissue mass arising from the anterior uterine wall (interstitial in location), measures about 12x11.5cm displays low signal intensity in T1WI.

**(C) Axial T2WI** displays mixed high and low signal intensity (central areas of high T2WI signal intensity consistent with degeneration)

**(D) Sagittal T1 fat sat post-contrast image** shows patchy heterogeneous enhancement of the mass compared to nearby myometrial tissue

**(E) DW-MRI with  $b = 1000 \text{ sec/ mm}^2$**  shows intermediate signal mass (Free diffusion)

(F)ADC map image demonstrates intermediate signal on the corresponding ADC map with ADC value ( $1.912 \times 10^{-3} \text{mm}^2/\text{s}$ ).

**Radiological diagnosis:**

Benign looking uterine lesion likely interstitial uterine fibroid.

**Pathological diagnosis:**

Confirmed to be interstitial uterine fibroid with mild hyaline degeneration.

UNDER PEER REVIEW